Published in final edited form as:

FASEB J. 2020 January ; 34(1): 1679–1694. doi:10.1096/fj.201900567RR.

Pharmacological inhibition of CSF1R by GW2580 reduces microglial proliferation and is protective against neuroinflammation and dopaminergic neurodegeneration

Matthew L. Neal[1,2], **Sheila M. Fleming**[2], **Kevin M. Budge**[3], **Alexa M. Boyle**[2,3], **Chunki Kim**[1], **Gelareh Alam**[2], **Eric E. Beier**[4], **Long-Jun Wu**[5], **Jason R. Richardson**[1,2,4]

[1]Department of Environmental Health, Robert Stempel School of Public Health and Social Work, Florida International University, Miami, FL, USA

[2]Department of Pharmaceutical Sciences and Center for Neurodegenerative Disease and Aging, Northeast Ohio Medical University, Rootstown, OH, USA

[3]Department of Biomedical Sciences, Kent State University, Kent, OH, USA

[4]Environmental and Occupational Health Sciences Institute, Rutgers University, Piscataway, NJ, USA

[5]Department of Neurology, Mayo Clinic, Rochester, MN, USA

Abstract

Increased pro-inflammatory cytokine levels and proliferation of activated microglia have been found in Parkinson's disease (PD) patients and animal models of PD, suggesting that targeting of the microglial inflammatory response may result in neuro-protection in PD. Microglial proliferation is regulated by many factors, but colony stimulating factor-1 receptor (CSF1R) has emerged as a primary factor. Using data mining techniques on existing microarray data, we found that mRNA expression of the CSF1R ligand, CSF-1, is increased in the brain of PD patients compared to controls. In two different neurotoxic mouse models of PD, acute MPTP and sub-chronic LPS treatment, mRNA and protein levels of CSF1R and CSF-1 were significantly increased. Treatment with the CSF1R inhibitor GW2580 significantly attenuated MPTP-induced CSF1R activation and Iba1-positive cell proliferation, without a reduction of the basal Iba1-positive population in the substantia nigra. GW2580 treatment also significantly decreased mRNA levels of pro-inflammatory factors, without alteration of anti-inflammatory mediators, and significantly attenuated the MPTP-induced loss of dopamine neurons and motor behavioral deficits. Importantly, these effects were observed in the absence of overt microglial depletion,

Correspondence Jason R. Richardson, Department of Environmental Health, Robert Stempel School of Public Health and Social Work, Florida International University, 11200 SW 8th St. AHC5-515, Miami, FL 33199, USA. jarichar@fiu.edu.

AUTHOR CONTRIBUTIONS

M.L. Neal conceived and designed research, performed research, conducted data analysis, drafting of the manuscript; S.M. Fleming, K.M. Budge, A.M. Boyle, C. Kim, G. Alam, and E.E. Beier conducted experiments; L.J. Wu helped with data interpretation and critical revising; J.R. Richardson conceived and designed experiments, helped draft and revise the manuscript.

SUPPORTING INFORMATION

Additional supporting information may be found online in the Supporting Information section.

CONFLICT OF INTEREST

The authors further declare that they have no competing financial conflicts or other conflicts of interest.

suggesting that targeting CSF1R signaling may be a viable neuroprotective strategy in PD that disrupts pro-inflammatory signaling, but maintains the beneficial effects of microglia.

Keywords

microglia; neuroprotection; Parkinson's disease; proliferation

1 | INTRODUCTION

Microglia play a critical role in both the healthy and diseased brain,[1,2] including pruning synapses, phagocytosing cell debris, and performing immune surveillance.[3] Because microglia are the resident macrophages and primary immune cell in the brain, they rapidly respond to neuronal injury by proliferation and production of pro-inflammatory factors. Increased numbers of activated microglia are found in the nigrostriatal region in both PD patients and animal models of PD, along with increased inflammatory cytokines.[4-7] This increased neuroinflammation is thought to play a critical role in the pathogenesis of PD.[8,9] Therefore, dampening the inflammatory response through attenuation of microglial proliferation could potentially halt or slow PD disease progression.

Signaling of colony stimulating factor-1 (CSF-1 or M-CSF) or interleukin-34 (IL-34) through the colony stimulating factor-1 receptor (CSF1R), also known as CD115 or the cFMS receptor, induces the receptor to homodimerize and auto-phosphorylate at multiples sites. This results in down-stream signaling to promote the survival, differentiation, and proliferation of mononuclear phagocytes such as microglia.[10] Deficiency of *Csf1r,* or either of its cognate ligands *Csf1* or *IL-34,* leads to a significant reduction in microglial density in mice.[11–13] Additionally, CSF1R signaling increases production of pro-inflammatory cytokines in cultured human microglia[14] and the overexpression of CSF1R in cultured mouse microglia was shown to increase pro-inflammatory cytokine production.[15] Together, these data demonstrate that CSF1R is a pivotal regulator of both microglial proliferation and production of pro-inflammatory cytokines.

Various diseases including rheumatoid arthritis,[16] Alzheimer's disease (AD),[17] amyotrophic lateral sclerosis (ALS),[18] and prion disease[19] show an increase in either CSF1R or its ligands CSF-1 and IL-34. Although CSF-1 expression is increased in various neurodegenerative diseases, glial fibrillary acidic protein (GFAP)-driven overexpression of CSF-1 in astrocytes in vivo was shown to increase microglial cell number without induction of a basal pro-inflammatory phenotype.[20] CSF1R inhibition, using the selective pharmacological ATP competitive inhibitor GW2580, led to significant reduction in microglial proliferation, neuroinflammation, and disease pathology in AD, ALS, and prion disease models.[17–19] However, recent data demonstrate that ablation of microglia using the pharmacological receptor tyrosine kinase inhibitor of CSF1R and related kinases, PLX-3397, led to increased neurotoxicity and behavioral deficits in an mouse model of PD using acute treatment with the select dopaminergic neurotoxicant (MPTP),[21] indicating that complete removal of microglia leads to exacerbation of disease phenotype. Together, these studies demonstrate the complexity of the roles of CSF-1 and CSF1R in neurodegeneration

and raise significant questions as to the targeting of CSF1R as a potential therapeutic target in neurodegeneration.

To address these questions, we examined CSF1 and CSF1R expression in the substantia nigra (SN) and striatum in mined microarray data from control and PD subjects along with samples from two animal models of PD, acute MPTP and a sub-chronic lipopolysaccharide (LPS) administration. Our results demonstrate that CSF-1 mRNA is increased in PD patients and CSF1R signaling is increased in the acute MPTP and LPS models of PD. Inhibition of CSF1R signaling with the specific ATP-competitive CSF1R inhibitor GW2580 did not deplete microglia, but attenuated MPTP-induced microglial proliferation, overall inflammatory response, dopaminergic neurotoxicity, and behavioral effects. These results suggest that selective targeting of CSF1R signaling efficiently reduces microglial proliferation and pro-inflammatory signaling, leading to protection of dopamine neurons.

2 | MATERIALS AND METHODS

2.1 | Reagents and antibodies

HRP secondary antibodies were purchased from Bio-Rad (Hercules, CA, USA). The primary mouse monoclonal antibody for iNOS (Cat #: sc-7271) was obtained from Santa Cruz Biotechnology Inc (Santa Cruz, CA, USA). The chicken polyclonal GFAP antibody (Cat. #: ab4674) and the rabbit monoclonal anti-CSF1R antibody (Cat#: AB221684) were acquired from Abcam (Cambridge, MA, USA). The rabbit polyclonal Iba1 antibody (Cat. #: 019–19741) was obtained from Wako (Richmond, VA). The rabbit anti-TH polyclonal antibody was bought from Millipore (Cat#: AB152). The Pierce BCA protein assay kit (Cat#: P123225) and the mouse anti-Ki-67 antibody (Cat#: 550 609) were purchased from Fisher Scientific. MPTP (Cat #: M0896–100MG) and all other reagents were obtained from Sigma-Aldrich (St. Louis, MO, USA), unless otherwise indicated.

2.2 | Animal care and treatment paradigms

Ten to twelve-week-old C57BL/6J male mice were obtained from Jackson Laboratories. For the acute MPTP treatment, mice were randomly assigned and injected intraperitoneally (i.p.) every 2 hours for a total of 4 doses of 12 mg/kg MPTP in 100 μL PBS. Mice were sacrificed 2 or 7 days after the last treatment. For the repeated dose LPS model, 100 μL of LPS (from *Salmonella abortus equi S*-form, Enzo Life Sciences, Farmingdale, NY, USA; cat #: ALX-581–009-L001) at a dose of 1 mg/kg in 100 μL PBS was administered i.p. once a day for 4 consecutive days.[22] Animals were sacrificed at 1 day or weeks after the last dose of LPS. Animal handling and experiments were performed in accordance with the NIH Guide for the Care and Use of Laboratory Animals and approved by the animal care committee of Rutgers Robert Wood Johnson Medical School and Northeast Ohio Medical University.

2.3 | Data mining of CSF1R, CSF-1, and IL- 34 gene expression in human tissue

Human gene expression data for *CSF1R, CSF-1,* and *IL-34* were obtained from the NCBI gene expression omnibus (GEO), which is a public repository of gene expression profiles from high-throughput microarray experiments that has the option to data mine for specific genes of interest.[23] Data were mined from two studies that collected the SN of PD patients

(total n = 22 males and 9 females) along with age-matched controls (total n = 10 males and 7 females), using the Affymetrix gene chip microarray.[24–26] The GEO accession numbers for the referenced studies are GDS2821 and GDS3128. The gene expression results in GEO are expressed as arbitrary units in the GEO due to different preparations of samples and different analyses but correlate to levels of gene expression. To allow examination of relative expression for these genes between the two different datasets, the expression values were normalized to controls and analyzed by Welch's *t*-test to account for the different sample numbers and variances.

2.4 | Quantitative PCR

RT-PCR was performed using an all-in-one cDNA synthesis kit (Bimake, Houston, TX, USA; cat #: B24408) to convert RNA into cDNA. Expression levels were determined using real-time PCR with Bimake RT2 SYBR Green master mix (Cat #: B21203) and previously published primer sets that were checked with NCBI BLAST[17,27] (Supplemental Table 1). For normalization of each sample, the mouse genes *Gapdh* or *Rpl13a* were used as housekeeping genes. Empirically derived amounts of template were used to achieve maximum efficiency of the PCR reaction without enzyme inhibition. Dissociation curves and melting curves were run according to manufacturer's guidelines to ensure that single amplicon peaks were obtained without any non-specific amplification. The $\Delta\Delta^{Ct}$ method was used to report the results as fold change using the threshold cycle (Ct) value for the housekeeping gene and for the respective gene of interest in each sample.

2.5 | Western blotting

Striatal tissue was homogenized, lysed by sonication, and run for western blotting as previously described.[22] Briefly, mouse striatum samples were homogenized using a handheld tissue grinder then sonicated using a microtip for 4–6 seconds. Cell debris was pelleted and removed, then samples were centrifuged for 45 minutes at 14 000 rpm to obtain the protein pellet. The supernatant was removed and retained, and protein was measured using a BCA kit. Equal amounts of protein were loaded for each sample onto precast gradient gels (Bio-Rad). Proteins were transferred to PVDF membranes using the iBlot2 semi-wet transfer instrument. Blots were blocked with 5% non-fat milk for 1 hour, then incubated in primary antibody overnight at 4°C. After washing the blot with Tris-buffered saline with Tween-20 (TBST), blots were incubated with HRP-conjugated secondary antibody for 1 hour in 5% milk. After washing with TBST, followed by deionized pure water, SuperSignal West Dura extended duration substrate (Thermo Fisher cat#: 34076) was added to the blot for 2 minutes, then imaged using the Protein Simple FluoChem E imaging system (Protein Simple; San Jose, CA, USA). Quantification of the protein bands was performed in ImageJ software and represented as percent control.

2.6 | Immunohistochemistry and unbiased stereology

Immunohistochemistry was performed as previously described.[27] Briefly, MPTP and LPS posttreatment brains were drop-fixed in 4% paraformaldehyde for 7 days. After 7 days, brains were washed with PBS, and placed into a 30% sucrose solution for at least 24 hours. The brains were then flash frozen with crushed dry ice and were sectioned at 40μm on a Thermo scientific Microm HM 450 sliding microtome with dry ice, and the sections were

placed into Cryosolution (30% sucrose, ethylene glycol, and PBS). Sections were washed with PBS and permeabilized with blocking buffer (2% bovine serum albumin (BSA), 0.1% Triton X-100, and Tween) for 1 hour at room temperature. Antibodies directed to the protein of interest were incubated with the sections overnight at 4°C in 2% BSA. The sections were probed with Alexa Fluor dye-conjugated goat secondary antibodies (1:1500) for 1 hour at room temperature. After washing with PBS, sections were mounted on slides using the Molecular Probes ProLong GOLD anti-fade mounting medium containing DAPI stain according to the manufacturer's instructions. Sections were imaged using the Leica TCS SPE confocal microscope.

DAB immunostaining was performed as previously described.[28] Briefly, endogenous peroxidases were quenched in 40 μm sections by 75% methanol and 2.5% H_2O_2 and sections were blocked (4% normal serum, 0.6% Triton X-100, and 5% BSA in 1×-PBS) and incubated with either rabbit anti-TH polyclonal antibody at 1:1000, rabbit anti-Iba1 antibody at 1:800, or chicken anti-GFAP antibody at 1:1000 for 24 hours at 4°C. The sections were then incubated with the biotinylated secondary antibody of goat anti-rabbit, or goat anti-chicken (Vector laboratory, Burlingame, CA, USA) for 1 hour at a 1:500 dilution followed by avidin-peroxidase complex. DAB substrate was used as the chromogen. Nissl staining was performed on neighboring sections with 0.5% cresyl violet according to our previous studies.[28]

Unbiased stereological counting was performed on a series of sections throughout the substantia nigra pars compacta (SNpc), choosing every 4th section throughout the nigra for a total of 8 sections. Cell counting was performed on the Leica DM 2500 LED microscope and Microbrightfield Stereo Investigator software (MBF Bioscience, Williston, VT, USA). TH-positive and Nissl-positive cell counts were performed on both hemispheres for each section. Borders of the SNpc were determined using a 5× objective and then cells were counted at 40× magnification. The SRS grid of 100 μm × 100 μm and a counting frame of 70 μm × 70 μm with a dissector height of 10 μm and 2 μm guard zones on either side were chosen. The coefficient error for all the animals counted was below 0.1 and a minimum of 300 markers were counted within 25–50 framing sites for each animal.

Quantification of CSF1R and iNOS immunofluorescence, along with Iba1-positive, GFAP-positive, and Ki-67-positive cell counts was performed using ImageJ analysis software. Cell counts were obtained from at least three fields for each section and three different sections for each treatment. At least three animals were analyzed for each treatment. Image quantifications were conducted without altering brightness or contrast. Representative images were treated equally for brightness and contrast alterations in ImageJ to increase immunoreactivity visualization.

2.7 | Motor behavioral analyses

Motor performance and coordination were determined by the challenging beam traversal task and performed as previously described.[29–31] Briefly, the beam consists of four sections (25 cm each, 1 m total length) with each section having a different width. The beam width begins at 3.5 cm and gradually narrows to 0.5 cm by 1 cm increments. Animals were trained to traverse the length of the beam starting at its widest section and ending at the narrowest

section. Mice received 2 days of training prior to testing; on the day of the test, a mesh grid (1 cm squares) of corresponding width was placed over the beam surface leaving an approximate 1 cm space between the grid and the beam surface. Animals were then recorded while traversing the grid-surfaced beam for five trials. Videos were viewed and rated on slow motion by an experimenter blind to treatment. Beam measurements included time to traverse, number of steps made by each animal, and stepping errors. Each mouse was scored using the mean of the five separate trials.

A small transparent cylinder (height, 15.5 cm, diameter, 12.7 cm) was used to measure spontaneous movement.[29–31] The cylinder was placed on a piece of glass with a mirror positioned at an angle beneath the glass to allow a clear view of movements along the ground and walls of the cylinder. Animals were recorded for three minutes and videos were viewed and rated in slow motion by an experimenter blind to treatment. The number of rears, forelimb, and hindlimb steps was measured.

2.8 | Data analysis

Data analyses were performed using the Prism 5.0 software package (GraphPad Software, San Diego, CA, USA). The data were first analyzed using a one-way ANOVA and then Tukey's posthoc test was performed to compare all treatment groups. Student's t-test was used when two groups were being compared, with the exception of the human gene expression data that were analyzed by Welch's *t*-test. All assays and tests were performed with 2–3 independent experimental repeats.

3 | RESULTS

3.1 | Levels of CSF1R and its cognate ligands CSF-1 and IL-34 in postmortem PD patients

Recently, increased *CSF1R* and *CSF-1* mRNA levels were found in the brain of AD patients[14,17] We hypothesized that CSF1R and its cognate ligands would similarly be increased in the brain of PD patients compared to age-matched controls. Using data from the gene expression omnibus at NCBI consisting of two different microarray studies of PD (n = 22 males and 9 females) and control brains (n = 10 males and 7 females),[25,26,32] we examined gene expression data of CSF1R and its cognate ligands, CSF1 and IL-34. *CSF1R* expression was increased by 15% in PD patients compared to control, but this increase was not statistically significant ($P = .18$; Figure 1A). However, gene expression of *CSF-1* was significantly increased by 26% in PD patients compared to control ($P = .033$, Figure 1B). The gene expression of the other cognate ligand for *CSF1R, IL-34,* was not different between the PD patients and control samples ($P = .997$, Figure 1C). These results indicate that CSF1R signaling, via increased levels of the CSF-1 ligand, may be present in PD patients, even in later stages of the disease, similar to that found in Alzheimer's disease postmortem patients.[14,17]

3.2 | Gene expression of CSF1R and its cognate ligands are induced in the striatum following LPS or MPTP treatment

We next examined CSF1R, CSF-1, and IL-34 levels in neurotoxic animal models of PD. Because CSF1R signaling is involved in microglial proliferation and inflammatory response,

we chose a common animal model of inflammation, using treatment with the potent inflammogen lipopolysaccharide (LPS; *Salmonella abortus equi* S-form), which induces neuroinflammation and dopaminergic neurodegeneration.[33,34] Our laboratory has previously characterized the microglial inflammatory response time course using this paradigm, and found the highest levels of pro-inflammatory factors 1 day after the last LPS injection, and by two weeks after the last LPS injection, the inflammatory response has returned to normal levels.[22] Here, striatal *Csf1r* mRNA was significantly increased by fourfold over saline-treated animals (Figure 1D) 1 day after the last LPS injection. Similarly, mRNA levels of both *Csf-1* and *Il-34* were significantly increased over saline-treated animals following the last LPS injection, with a three-fold and two-fold higher expression levels, respectively (Figure 1D). Two weeks following the last injection of LPS, which is a time point that has demonstrated significant neurodegeneration and reduced inflammatory status,[22] the mRNA levels for *Csf1r*, *Csf-1,* and *Il-34* returned to near control levels.

In the acute MPTP model (four injections of 12 mg/kg once every 2 hours), *Csf1r* mRNA levels were increased by almost threefold over the saline 2 days following treatment (Figure 1E). *Csf-1* gene expression was also increased over twofold higher than saline-treated animals at this time point (Figure 1E). However, *Il-34* mRNA levels did not change following MPTP treatment (Figure 1E). Expression of *Csf1r, Csf-1*, and *Il-34* returned to control levels 7 days following MPTP treatment, which corresponds to the time point of significant neurotoxicity and reduced inflammatory status.[22,35] Taken together, these data indicate that mRNA levels of *Csf1r* and its cognate ligands are induced at early time points during peak inflammatory response in both LPS and MPTP animal models of PD.

3.3 | CSF1R and CSF-1 protein levels are increased in the nigrostriatal regions following neurotoxicant treatment

To verify the gene expression results post LPS treatment, we examined the protein level of CSF1R in both the striatum and SN, one day after the last LPS injection. Western blot analysis of striatal CSF1R protein levels followed the same trend as the mRNA results, with CSF1R levels significantly increased by over 250% in the striatum following LPS treatment compared to saline-treated animals (Figure 2A). Similarly, immunofluorescence of CSF1R in the SN was visibly increased after injection of LPS (Figure 2B).

Next, we examined the protein level of CSF1R 2 days following acute MPTP treatment using western blotting in the striatum and using immunofluorescence in the SN to verify the gene expression results. Similar to the mRNA results found by qPCR, CSF1R protein levels in the striatum were significantly higher, with an average of 200% increase compared to saline-treated animals (Figure 2C). Acute MPTP treatment visibly induced CSF1R immunofluorescence over saline-treated animals in the SN 2 days after MPTP injection (Figure 2D). Because neurons can also express CSF1R,[36] immunofluorescent microscopy was used to examine the cell-type-specific increase in CSF1R. Following either LPS or MPTP treatment, CSF1R protein levels were increased in Iba1-positive cells of the SN (Figure 2B,D), with very little expression and upregulation of CSF1R in TH-positive neurons (Supplemental Figure 1).

Because we found that CSF-1 gene expression is increased in PD patients compared to age-matched controls and in both the MPTP and LPS neurotoxicant animal models of PD, we wanted to investigate whether the CSF-1 protein was also increased in the SN following MPTP treatment. CSF-1 protein levels were significantly increased in the striatum 2 days after MPTP treatment (Figure 2E), and visibly increased in the SN (Figure 2F). However, the majority of CSF-1 immunofluorescence did not colocalize with Iba1-positive cells (Figure 2F).

3.4 | Pharmacological inhibition of CSF1R attenuates MPTP-induced microglial proliferation

Targeting of CSF1R by pharmacological agents has led to mixed results, with PLX-3397 leading to ablation of microglia and enhancement of MPTP-induced neurotoxicity,[21] while the selective pharmacological ATP competitive inhibitor GW2580 was shown to not ablate microglia and decrease neurotoxicity in animal models of AD, ALS, and prion disease.[17–19] Here, we administered GW2580 by oral gavage (80 mg/kg) 2 hours after the final MPTP injection and every 12 hours thereafter until the animals were sacrificed 2 days later (Figure 3A). GW2580 was given 2 hours after the last MPTP injection to avoid any interactions between the two drugs, because peak levels of MPP+ levels from metabolized MPTP occur within 2 hours.[37]

To determine whether GW2580 would inhibit MPTP-induced activation of CSF1R and subsequent microglial proliferation, we assessed phosphorylated CSF1R (pCSF1R) in Iba1-positive cells in the SN. After ligand binding, CSF1R auto-phosphorylates itself at multiple sites, one of which is tyrosine 271 (Y271) in mice, leading to downstream signaling pathways such as PI3K and AKT.[38] MPTP treatment increased pCSF1R levels, and GW2580 treatment abolished this increase. Immunofluorescent images demonstrate that GW2580 treatment alone visibly decreased the levels of Y271 compared to saline (Figure 3B) and led to a 12% reduction in basal Iba1-positive cell (Figure 3E), but this was not a statistically significant decrease. A reduction of the basal number of microglia from GW2580 alone is expected due to the inhibition of basal microglial proliferation, but this dose and treatment paradigm of GW2580 does not appear to ablate microglia.

To further assess the effects of MPTP and GW2580 on the resident microglial population, we determined gene expression of the macrophage and microglial marker Iba1 (gene name *Aif1*), along with counting the number of Iba1-positive cells in the SN. Acute MPTP treatment significantly induced *Aif1* mRNA levels in the striatum compared to saline-treated animals (Figure 3C). Similarly, DAB immunostaining in the SN for Iba1 revealed that the acute MPTP treatment induced a significant ~ twofold increase in total number of Iba1-positive cells compared to saline-treated animals. The increase in Iba1-positive cell numbers was almost completely abolished with GW2580 (Figure 3D). GW2580 treatment did not result in ablation of the existing microglial population, with Iba1 gene expression and Iba1-positive counts at the same level as that of saline-treated animals. Further, the Iba1-positive cells in animals treated with MPTP and GW2580 exhibited hypertrophy and thickened processes, which are indicative of an activated state, and demonstrate that these microglia can respond to a stimulus. To confirm that GW2580 prevented microglial proliferation, we

probed sections with an antibody to the proliferation marker Ki-67 and co-labeled with Iba1. MPTP significantly increased the number of Iba1-positive cells labeled with Ki-67 and GW2580 treatment almost completely abolished this increase (Figure 3E,F). The Iba1 immunofluorescence confirmed our prior result that GW2580 did not ablate the basal microglial population, although there was around 12% reduction in the number of Ki-67-positive cells also positive for Iba1 following GW2580 treatment (Figure 3F,G). These results show that GW2580 attenuates the MPTP-induced microglial proliferation, while not ablating the basal microglial population.

3.5 | Pharmacological inhibition of CSF1R attenuates MPTP-induced neuroinflammation without altering astrocyte reactivity

Olmos-Alonso et al found that GW280 reduced expression of both CSF1R and CSF-1 in the brains of transgenic mouse models of Alzheimer's disease.[17] To assess whether GW2580 treatment alters the levels of CSF1R, CSF-1, or IL-34, we utilized qPCR to examine mRNA expression levels of *Csf1r*, *Csf1*, and *Il-34* in the mouse striatum following GW2580 treatment with or without MPTP exposure. Similar to results from Figure 2, we found that MPTP treatment significantly increased CSF1R mRNA levels and increased CSF-1, with no change in IL-34 levels (Figure 4A). GW2580 significantly reduced the levels of Csf1r mRNA following MPTP treatment, indicating that inhibiting CSF1R signaling either reduces CSF1R gene expression or results from a reduced population of microglia. There were no statistically significant differences with GW2580 for *Csf1* or *Il34*, however, there was a trend for reduced expression for both factors.

To determine whether the attenuation of microglial proliferation leads to significant reduction in the MPTP-induced neuroinflammation, we assessed several markers of pro-inflammatory and anti-inflammatory microglia. MPTP treatment significantly increased the gene expression of the pro-inflammatory factors *Nos2*, *Gp91phox*, *Il-6,* and *Il-1b* in the mouse striatum 2 days following the MPTP treatment (Figure 4A). GW2580 treatment in the MPTP mice resulted in decreased *Il-1b* (Figure 4A) and a significant decrease in the gene expression of *Nos2*, *Gp91phox*, and *Il-6* (Figure 4A). In contrast, MPTP treatment did not increase any of the measured anti-inflammatory genes *Arginase-1*, *Ym1*, *Nrf2*, and *Mrc1*, but reduced gene expression of several of these, but only *Mrc1* was significant expression (Figure 4B). GW2580 treatment alone or following MPTP injections did not reduce expression of the M2 genes, and significantly attenuated MPTP-reduced *Mrc1* expression.

A recent study demonstrated that ablation of microglia using the CSF1R and related kinase inhibitor PLX3397 led to increased astrocyte reactivity and inflammatory response, but did not increase the total number of astrocytes.[21] Therefore, we investigated whether GFAP-positive astrocytes were altered following GW2580 treatment with or without MPTP. GW2580 did not alter the basal number of GFAP-positive cells following MPTP and GW2580 treatment (Figure 5A,B). To further confirm that GW2580 treatment does not increase astrocyte reactivity or the astrocyte inflammatory response, we utilized immunohistochemistry to visualize iNOS protein levels in GFAP-positive cells of the SN (Figure 5C). MPTP treatment visibly increased the iNOS protein level in GFAP-positive cells compared to saline-treated animals, but GW2580 did not lead to a visible change in

iNOS protein level with or without MPTP treatment. These data indicate that inhibition of microglial proliferation by GW2580 did not have a significant effect on the basal astrocyte population or exacerbate the astrocyte inflammatory response following MPTP treatment.

3.6 | Pharmacological inhibition of CSF1R attenuates MPTP-induced dopaminergic neurodegeneration and behavioral deficits

The major pathological characteristic of PD is the loss of dopaminergic neurons in the SN region of the brain, and the acute MPTP model has been well characterized to induce dopaminergic neurotoxicity.[39] The same MPTP and GW2580 paradigm was used and mice were sacrificed 7 days following the MPTP injections (Figure 6A). To measure dopaminergic neurotoxicity, we used TH DAB immunostaining (Figure 6B) and Nissl staining followed by unbiased stereology to count the total TH-positive and Nissl-positive neurons in the SN. Acute MPTP treatment significantly reduced the number of TH-positive neurons to 60% of control (Figure 6C) and Nissl-positive neurons to 61% (Figure 6D). GW2580 treatment significantly attenuated the loss of both TH+ and Nissl+ neurons, with 18% and 17% loss compared to control, respectively (Figure 6C,D).

Several behavioral tests were used to determine whether the attenuation of MPTP-induced neurotoxicity by GW2580 treatment led to protection from behavioral deficits. First, mice were tested on the challenging beam, a raised beam that reduces in width as it gets closer to the platform.[29–31] On the challenging beam, mice are tested for the time it takes to cross the beam and how many errors were committed while crossing. MPTP treatment did not change the number of errors made by the mice as they crossed (data not shown), but it did significantly increase the amount of time it took for the mice to traverse the beam and the average time per step (Figure 6E,F). In MPTP-treated mice, GW2580 treatment significantly attenuated the increase in time taken to traverse the beam and average time per step (Figure 6E,F). Next, we measured the number of animal rears, along with the number of forelimb and hindlimb steps by imaging the mice from under a glass cylinder. MPTP treatment did not affect the number of forelimb steps (Figure 6G, left panel); however, there was a significant reduction in the number of rears and hindlimb steps in the MPTP-treated animals compared to the controls (Figure 6G, right panel). Treatment with GW2580 significantly attenuated the MPTP-induced reduction in hindlimb steps (Figure 6G) and number of rears (Figure 6H). Taken together, these data demonstrate that GW2580 inhibition of microglial proliferation, while not inducing ablation, can protect against MPTP-induced neurotoxicity and motor deficits.

3.7 | Discussion

Microglial proliferation, activation, and inflammatory response are thought to play a crucial role in the pathogenesis of PD.[4–7] Several studies show that activation of the CSF1R receptor is responsible for the increased microglial proliferation in AD, prion disease, and ALS.[17–19] Here, we provide novel evidence that CSF1R signaling may likewise contribute to microglial proliferation and neuroinflammation in PD, as evidenced by increased levels of the ligand CSF-1 in postmortem PD patients, along with increased mRNA and protein levels of CSF1R, CSF-1, and IL-34 in animal models of PD. Treatment with GW2580, an orally bioavailable selective CSF1R inhibitor, inhibited increased microglial proliferation without

ablation of microglia, and attenuated the MPTP-induced neuroinflammatory response, dopaminergic neurotoxicity, and behavioral deficits. These results support the notion that the inflammatory response and microglial proliferation are key mediators of dopaminergic neurotoxicity in PD.

Although an increased number of activated microglia has been observed in PD patients and animal models of PD,[40–43] this is the first study to investigate the levels of CSF1R and its cognate ligands, which are key mediators of microglial proliferation, in the brain of PD patients and two neurotoxic animal models of PD. We started our investigation of CSF1R, CSF-1, and IL-34 by data mining the NCBI GEO, which is a free repository of curated gene expression results. We found that samples from PD patients had higher gene expression of CSF1R and significantly higher CSF-1 gene expression compared to age-matched controls, whereas IL-34 was not different between the groups (Figure 1). The lack of a significant increase of CSF1R in the postmortem PD patients could be due to the role of CSF1R in the early inflammatory response of microglia with the mRNA levels potentially peaking earlier in the disease. We tested this hypothesis by utilizing an LPS inflammation model and an acute MPTP neurotoxicity model. The increased mRNA and protein levels of CSF1R and CSF-1 in both PD animal models corresponded to the time points of peak inflammatory response,[22,35] and returned to control levels at later timepoints. In general, our data correspond to those found in the brain of postmortem AD patients, with CSF1R and CSF-1 levels increased.[14] IL-34 gene expression was significantly increased with LPS treatment, but not with MPTP treatment, indicating a differential regulation of the two ligands. CSF-1 and IL-34 both bind to CSF1R and are both expressed in the brain, but the cell signaling events differ between the two ligands.[44,45] We observed increased CSF-1 mRNA levels in the brains of PD patients compared to age-matched controls (Figure 1B), whereas we found no difference in IL-34 mRNA levels (Figure 1C). Further, CSF-1 gene expression and protein levels were increased in the SN in animal models of PD, suggesting that CSF-1 is the pre-dominant factor in PD. However, the cells producing the increased CSF-1 are still unknown in these models of PD and could be from microglia, astrocytes, and neurons.[46–48] Similar to results found by Olmos-Alonso et al,[17] GW2580 treatment in this study caused a significant reduction in CSF1R. Therefore, future studies using GW2580 could examine the cell-type-specific expression of CSF-1 in PD models.

Regulation of microglial proliferation and the potential of microglial ablation to slow or stop the progression of neurodegeneration has recently become an active area of study, utilizing various CSF1R inhibitors to study the role of either microglial proliferation or complete microglial ablation in models of neurodegenerative diseases. PLX-3397 is a commonly used pharmacological inhibitor that completely ablates microglia or macrophage populations, which is accomplished by inhibiting CSF1R along with other kinases in the same family, including c-kit, PDGFRβ, and FTL3.[49] Class III receptor tyrosine kinases, which includes CSF1R, c-kit, PDGFRβ, and FLT3, all regulate cell survival through downstream pathways such as PI3K and Akt. Inhibition of CSF1R individually would still allow the other class III receptors to promote survival, but inhibition of multiple or all of these receptor kinases using a pharmaceutical inhibitor such as PLX-3397 leads to ablation of macrophages and microglia.[21,50,51] Recent research found that complete ablation of microglia in the brain using PLX-3397 exacerbated MPTP-induced neuroinflammation, neurotoxicity, and

behavioral effects.[21] These results demonstrate that complete removal of the basal microglial population could lead to detrimental effects. Here, we utilized GW2580, which has a much higher affinity for CSF1R and prevents its activation without inhibition of related kinases or result in ablation of the macrophage or microglial population.[17–19] GW2580 completely blocked the MPTP-induced gene expression of Iba1 in the mouse striatum, along with significant reduction of Iba1+ and Ki-67+/ Iba1+ cells in the SN (Figure 4). This was accompanied by reduced levels of phosphorylated CSF1R, without a significant reduction of the basal microglial population, indicating that GW2580 primarily blocks the activation of CSF1R. The discrepancies among the different inhibitors are likely related to the dose and treatment duration. For instance, BLZ945 is highly specific for CSF1R with an IC50 about 1nM, but can also inhibit c-kit (3.2μM) and PDGFR-β (4.8μM) at higher concentrations.[52] Similarly, GW2580 has an IC50 for CSF1R around 10 nM,[53] but can also inhibit TRKA around 88 nM.[54] Therefore, activity for related kinases along with dose of CSF1R inhibitors appears to be an important factor in determining significant off-target or enhanced target-mediated effects and could explain variation in experimental results between studies. Future studies could investigate the comparison between GW2580 and PLX-3397 in various animal models of PD and other neurodegenerative diseases to investigate the impact of microglial ablation vs CSF1R inhibition without microglial ablation.

Reducing the inflammatory response is protective in animal models of PD.[55,56] We found that treatment with GW2580 significantly attenuated the MPTP-induced striatal tissue mRNA levels of the pro-inflammatory factors *Nos2, Gp91phox, Il-6,* and *Il-1b*. Although the reduced tissue inflammatory response is most likely attributable to attenuation of MPTP-induced microglial proliferation, which is evident from the reduction in Ki-67+/Iba1+ cells, CSF1R inhibition may also directly mitigate pro-inflammatory cell signaling. Some evidence indicates that CSF1R inhibition reduces expression of pro-inflammatory factors along with inhibiting proliferation.[16–18] Walker et al found that cultured human microglia stimulated with CSF-1 or IL-34 resulted in increased gene expression of pro-inflammatory cytokines such as *IL-1b*, *TNFa,* and *IL-6* along with pro-inflammatory signaling factors such as STAT1.[14] Therefore, CSF1R inhibition may reduce microglial inflammatory response even after proliferation has occurred through dampening production of inflammatory factors such as IL-1β, TNFα, and IL-6. One study found that inhibiting mitotic cell division using AraC given by osmotic pump directly into the brain significantly attenuated microglial proliferation following prion exposure, but also led to an increased inflammatory profile in the microglia.[19] These studies provide evidence that CSF1R inhibition could be through reducing both the microglial proliferation and the inflammatory response of these cells in PD models. Further, in this study, we found that Iba1+ cells in the MPTP + GW2580 group exhibited hypertrophy, or enlarged cell bodies, and thickened processes, which indicate some degree of microglial activation. Therefore, the microglial population following GW2580 treatment still demonstrates the ability to become activated to a neurotoxic stimulus, but potentially to a lesser extent.

Complete ablation of microglia using PLX-3397 in an MPTP mouse model led to exacerbated astrocyte reactivity,[21] which indicates that a basal microglial population is necessary to limit astrocyte reactivity. In our study, we found that GW2580 treatment significantly attenuated MPTP-induced overall striatal inflammatory factor gene expression

and did not alter the astrocyte population with or without MPTP treatment (Figure 4C-E). Similarly, we went on to demonstrate that GW2580 did not alter the basal iNOS protein level in GFAP-positive cells of the SN or following MPTP treatment. Reactive astrocytes can exacerbate neurotoxicity and can propagate the immune response by inducing infiltration of peripheral immune cells,[57] therefore it is important that CSF1R inhibition with GW2580 did not increase astrocyte reactivity with or without MPTP treatment. Further, the attenuated *Nos2* mRNA levels from Figure 4B would most likely arise from the reduced microglial proliferation following MPTP, since astrocyte iNOS levels were not significantly different in the MPTP + GW2580 treatment group. Although we cannot rule out the role of infiltrating peripheral monocytes or neutrophils in this study, a previous group found that peripheral macrophage infiltration does not influence neurotoxicity in the acute MPTP model.[58]

We found significant loss of the TH+ and Nissl+ neurons in the SN of mice treated with acute MPTP (Figure 6C,D), demonstrating neuronal cell death and not loss of TH expression.[28] Further, mice treated with MPTP exhibited significant motor deficits compared to saline-treated mice. GW2580 treatment significantly abolished the MPTP-induced loss of both the TH+ and Nissl+ cells, along with partially rescuing MPTP-induced deficits in traversing a challenging beam and in spontaneous movements (Figure 6E–H). This is concurrent with literature demonstrating beneficial results with GW2580 treatment in animal models of AD, prion disease, and ALS.[17–19] The neuroprotection is most likely through the reduction of microglial proliferation and inflammatory response; however, CSF1R has also been found in neurons. In fact, one study found that direct CSF-1 or IL-34 signaling through CSF1R is neuroprotective in both the hippocampus and cortex.[36] Here, we found that increased CSF1R levels were almost exclusively found in microglia, similar to findings in the spinal cord of an ALS mouse model.[18] Together, these data demonstrate that neuroprotection by GW2580 inhibition of CSF1R signaling is likely mediated through microglia.

Studies investigating CSF1R signaling in neurodegeneration have produced mixed results, revealing that this is a complex signaling mechanism in neurodegenerative diseases. More studies are needed to determine the potential systemic effect, including overall immune system function, of using a CSF1R inhibitor such as GW2580, including chronic animal models of PD such as synuclein mutation or overexpression. Especially since two studies have found that CSF1R inhibition could specifically limit M2 macrophage numbers in systemic tissues.[59,60] However, several pharmacological inhibitors to CSF1R or related kinases have been tested in clinical trials and overt immune system dysfunction was not found.61 Similarly, another study found that giving GW2580 for 14 days did not reduce the number of peripheral blood monocytes.53 This study, along with previous studies that demonstrate the potential for targeted and mechanism-specific CSF1R inhibition in protecting against neurodegenerative diseases, human cancers, and rheumatoid arthritis, reveals the need to evaluate GW2580 or other selective CSF1R inhibitors as potential disease-modifying treatments in PD.

Supplementary Material

Refer to Web version on PubMed Central for supplementary material.

ACKNOWLEDGMENTS

This work was supported by National Institutes of Health grants T32ES007148, P30ES005022, R01ES021800, R01NS088627, and the Michael J Fox Foundation for Parkinson's Disease Research. Additional support was provided through generous donations from the Allan and Janice Woll Research Fund, the Richard Nicely Parkinson's Research Fund and the Glenn and Karen Leppo Parkinson's Research Fund. The content of this article is solely the responsibility of the authors and does not necessarily represent the official views of any of the funding contributors. The funding agencies had no role in the study design, conduct, interpretation, or decision to publish this study.

Funding information

HHS | NIH | National Institute of Environmental Health Sciences (NIEHS), Grant/Award Number: R01ES021800; HHS | NIH | National Institute of Neurological Disorders and Stroke (NINDS), Grant/ Award Number: R01NS088627

Abbreviations:

AD	Alzheimer's disease
ALS	amyotrophic lateral sclerosis
CSF1R	colony stimulating factor 1 receptor
CSF-1	colony stimulating factor 1
DAB, 3,3'	diaminobenzidine
GEO	gene expression omnibus
GFAP	glial fibrillary acidic protein
Iba1	ionized calcium-binding adaptor molecule
IL-34	interleukin-34; LPS, lipopolysaccharide
MPTP	1-methyl-4-phenyl-1,2,3,6-tetrahydropyridine
MPP+	1-methyl-4-phenylpyridinium
PD	Parkinson's disease
SN	substantianigra
TH	tyrosine hydroxylase

REFERENCES

1. Frost JL, Schafer DP. Microglia: architects of the developing nervous system. Trends Cell Biol. 2016;26:587–597. [PubMed: 27004698]
2. Eyo UB, Wu LJ. Bidirectional microglia-neuron communication in the healthy brain. Neural Plast. 2013;2013:456857. [PubMed: 24078884]

3. Wake H, Moorhouse AJ, Nabekura J. Functions of microglia in the central nervous system–beyond the immune response. Neuron Glia Biol. 2011;7:47–53. [PubMed: 22613055]
4. Imamura K, Hishikawa N, Sawada M, Nagatsu T, Yoshida M, Hashizume Y. Distribution of major histocompatibility complex class II-positive microglia and cytokine profile of Parkinson's disease brains. Acta Neuropathol. 2003;106:518–526. [PubMed: 14513261]
5. Hirsch EC, Hunot S. Neuroinflammation in Parkinson's disease: a target for neuroprotection? Lancet Neurol. 2009;8:382–397. [PubMed: 19296921]
6. Sriram K, Matheson JM, Benkovic SA, Miller DB, Luster MI, O'Callaghan JP. Deficiency of TNF receptors suppresses microglial activation and alters the susceptibility of brain regions to MPTP-induced neurotoxicity: role of TNF-alpha. FASEB J. 2006;20:670–682. [PubMed: 16581975]
7. Whitton PS. Inflammation as a causative factor in the aetiology of Parkinson's disease. Br J Pharmacol. 2007;150:963–976. [PubMed: 17339843]
8. Zhang W, Wang T, Pei Z, et al. Aggregated alpha-synuclein activates microglia: a process leading to disease progression in Parkinson's disease. FASEB J. 2005;19:533–542. [PubMed: 15791003]
9. Zhang QS, Heng Y, Yuan YH, Chen NH. Pathological α-synuclein exacerbates the progression of Parkinson's disease through microglial activation. Toxicol Lett. 2017;265:30–37. [PubMed: 27865851]
10. Hume DA, MacDonald KP. Therapeutic applications of macrophage colony-stimulating factor-1 (CSF-1) and antagonists of CSF-1 receptor (CSF-1R) signaling. Blood. 2012;119:1810–1820. [PubMed: 22186992]
11. Erblich B, Zhu L, Etgen AM, Dobrenis K, Pollard JW. Absence of colony stimulation factor-1 receptor results in loss of microglia, disrupted brain development and olfactory deficits. PLoS ONE. 2011;6:e26317. [PubMed: 22046273]
12. Kondo Y, Duncan ID. Selective reduction in microglia density and function in the white matter of colony-stimulating factor-1-deficient mice. J Neurosci Res. 2009;87:2686–2695. [PubMed: 19396881]
13. Greter M, Lelios I, Pelczar P, et al. Stroma-derived interleukin-34 controls the development and maintenance of langerhans cells and the maintenance of microglia. Immunity. 2012;37:1050–1060. [PubMed: 23177320]
14. Walker DG, Tang TM, Lue LF. Studies on colony stimulating factor receptor-1 and ligands colony stimulating factor-1 and interleukin-34 in Alzheimer's disease brains and human microglia. Front Aging Neurosci. 2017;9:244. [PubMed: 28848420]
15. Mitrasinovic OM, Perez GV, Zhao F, Lee YL, Poon C, Murphy GM. Overexpression of macrophage colony-stimulating factor receptor on microglial cells induces an inflammatory response. J Biol Chem. 2001;276:30142–30149. [PubMed: 11387343]
16. Garcia S, Hartkamp LM, Malvar-Fernandez B, et al. Colony-stimulating factor (CSF) 1 receptor blockade reduces inflammation in human and murine models of rheumatoid arthritis. Arthritis Res Ther. 2016;18:75. [PubMed: 27036883]
17. Olmos-Alonso A, Schetters ST, Sri S, et al. Pharmacological targeting of CSF1R inhibits microglial proliferation and prevents the progression of Alzheimer's-like pathology. Brain. 2016;139:891–907. [PubMed: 26747862]
18. Martínez-Muriana A, Mancuso R, Francos-Quijorna I, et al. CSF1R blockade slows the progression of amyotrophic lateral sclerosis by reducing microgliosis and invasion of macrophages into peripheral nerves. Sci Rep. 2016;6:25663. [PubMed: 27174644]
19. Gómez-Nicola D, Fransen NL, Suzzi S, Perry VH. Regulation of microglial proliferation during chronic neurodegeneration. J Neurosci. 2013;33:2481–2493. [PubMed: 23392676]
20. De I, Nikodemova M, Steffen MD, et al. CSF1 overexpression has pleiotropic effects on microglia in vivo. Glia. 2014;62:1955–1967. [PubMed: 25042473]
21. Yang X, Ren H, Wood K, et al. Depletion of microglia augments the dopaminergic neurotoxicity of MPTP. FASEB J. 2018; 32:3336–3345. 10.1096/fj.201700833RR. [PubMed: 29401614]
22. Beier EE, Neal M, Alam G, Edler M, Wu LJ, Richardson JR. Alternative microglial activation is associated with cessation of progressive dopamine neuron loss in mice systemically administered lipopolysaccharide. Neurobiol Dis. 2017;108:115–127. [PubMed: 28823928]

23. Edgar R, Domrachev M, Lash AE. Gene Expression Omnibus: NCBI gene expression and hybridization array data repository. Nucleic Acids Res. 2002;30:207–210. [PubMed: 11752295]
24. Papapetropoulos S, Ffrench-Mullen J, McCorquodale D, Qin Y, Pablo J, Mash DC. Multiregional gene expression profiling identifies MRPS6 as a possible candidate gene for Parkinson's disease. Gene Expr. 2006;13:205–215. [PubMed: 17193926]
25. Moran LB, Duke DC, Deprez M, Dexter DT, Pearce RK, Graeber MB. Whole genome expression profiling of the medial and lateral substantia nigra in Parkinson's disease. Neurogenetics. 2006;7:1–11. [PubMed: 16344956]
26. Duke DC, Moran LB, Kalaitzakis ME, et al. Transcriptome analysis reveals link between proteasomal and mitochondrial pathways in Parkinson's disease. Neurogenetics. 2006;7:139–148. [PubMed: 16699787]
27. Neal ML, Boyle AM, Budge KM, Safadi FF, Richardson JR. The glycoprotein GPNMB attenuates astrocyte inflammatory responses through the CD44 receptor. J Neuroinflammation. 2018;15:73. [PubMed: 29519253]
28. Alam G, Edler M, Burchfield S, Richardson JR. Single low doses of MPTP decrease tyrosine hydroxylase expression in the absence of overt neuron loss. Neurotoxicology. 2017;60:99–106. [PubMed: 28377118]
29. Fleming SM, Salcedo J, Fernagut PO, et al. Early and progressive sensorimotor anomalies in mice overexpressing wild-type human alpha-synuclein. J Neurosci. 2004;24:9434–9440. [PubMed: 15496679]
30. Fleming SM, Mulligan CK, Richter F, et al. A pilot trial of the microtubule-interacting peptide (NAP) in mice overexpressing alpha-synuclein shows improvement in motor function and reduction of alpha-synuclein inclusions. Mol Cell Neurosci. 2011;46:597–606. [PubMed: 21193046]
31. Fleming SM, Santiago NA, Mullin EJ, et al. The effect of manganese exposure in Atp13a2-deficient mice. Neurotoxicology. 2018;64:256–266. [PubMed: 28595912]
32. Lesnick TG, Papapetropoulos S, Mash DC, et al. A genomic pathway approach to a complex disease: axon guidance and Parkinson disease. PLoS Genet. 2007;3:e98. [PubMed: 17571925]
33. Qin L, Wu X, Block ML, et al. Systemic LPS causes chronic neuroinflammation and progressive neurodegeneration. Glia. 2007;55:453–462. [PubMed: 17203472]
34. Catorce MN, Gevorkian G. LPS-induced murine neuroinflammation model: main features and suitability for pre-clinical assessment of nutraceuticals. Curr Neuropharmacol. 2016;14:155–164. [PubMed: 26639457]
35. Noelker C, Morel L, Lescot T, et al. Toll like receptor 4 mediates cell death in a mouse MPTP model of Parkinson disease. Sci Rep. 2013;3:1393. [PubMed: 23462811]
36. Luo J, Elwood F, Britschgi M, et al. Colony-stimulating factor 1 receptor (CSF1R) signaling in injured neurons facilitates protection and survival. J Exp Med. 2013;210:157–172. [PubMed: 23296467]
37. Fornai F, Alessandrì MG, Torracca MT, Bassi L, Corsini GU. Effects of noradrenergic lesions on MPTP/MPP+ kinetics and MPTP-induced nigrostriatal dopamine depletions. J Pharmacol Exp Ther. 1997;283:100–107. [PubMed: 9336313]
38. Sampaio NG, Yu W, Cox D, et al. Phosphorylation of CSF-1R Y721 mediates its association with PI3K to regulate macrophage motility and enhancement of tumor cell invasion. J Cell Sci. 2011;124:2021–2031. [PubMed: 21610095]
39. Meredith GE, Rademacher DJ. MPTP mouse models of Parkinson's disease: an update. J Parkinsons Dis. 2011;1:19–33. [PubMed: 23275799]
40. Langston JW, Forno LS, Tetrud J, Reeves AG, Kaplan JA, Karluk D. Evidence of active nerve cell degeneration in the substantia nigra of humans years after 1-methyl-4-phenyl-1,2,3,6-tetrahydro-pyridine exposure. Ann Neurol. 1999;46:598–605. [PubMed: 10514096]
41. Forno LS. Neuropathology of Parkinson's disease. J Neuropathol Exp Neurol. 1996;55:259–272. [PubMed: 8786384]
42. Knott C, Stern G, Wilkin GP. Inflammatory regulators in Parkinson's disease: iNOS, lipocortin-1, and cyclooxygenases-1 and −2. Mol Cell Neurosci. 2000;16:724–739. [PubMed: 11124893]

43. Marinova-Mutafchieva L, Sadeghian M, Broom L, Davis JB, Medhurst AD, Dexter DT. Relationship between microglial activation and dopaminergic neuronal loss in the substantia nigra: a time course study in a 6-hydroxydopamine model of Parkinson's disease. J Neurochem. 2009;110:966–975. [PubMed: 19549006]
44. Boulakirba S, Pfeifer A, Mhaidly R, et al. IL-34 and CSF-1 display an equivalent macrophage differentiation ability but a different polarization potential. Sci Rep. 2018;8:256. [PubMed: 29321503]
45. Nakamichi Y, Udagawa N, Takahashi N. IL-34 and CSF-1: similarities and differences. J Bone Miner Metab. 2013;31: 486–495. [PubMed: 23740288]
46. Takeuchi A, Miyaishi O, Kiuchi K, Isobe K. Macrophage colony-stimulating factor is expressed in neuron and microglia after focal brain injury. J Neurosci Res. 2001;65:38–44. [PubMed: 11433427]
47. Inden M, Kitamura Y, Takeuchi H, et al. Neurodegeneration of mouse nigrostriatal dopaminergic system induced by repeated oral administration of rotenone is prevented by 4-phenylbutyrate, a chemical chaperone. J Neurochem. 2007;101:1491–1504. [PubMed: 17459145]
48. Frei K, Nohava K, Malipiero UV, Schwerdel C, Fontana A. Production of macrophage colony-stimulating factor by astrocytes and brain macrophages. J Neuroimmunol. 1992;40: 189–195. [PubMed: 1430151]
49. Smith CC, Zhang C, Lin KC, et al. Characterizing and overriding the structural mechanism of the Quizartinib-resistant FLT3 "Gatekeeper" F691L mutation with PLX3397. Cancer Discov. 2015;5:668–679. [PubMed: 25847190]
50. Elmore MR, Lee RJ, West BL, Green KN. Characterizing newly repopulated microglia in the adult mouse: impacts on animal behavior, cell morphology, and neuroinflammation. PLoS ONE. 2015;10:e0122912. [PubMed: 25849463]
51. Dammeijer F, Lievense LA, Kaijen-Lambers ME, et al. Depletion of tumor-associated macrophages with a CSF-1R kinase inhibitor enhances antitumor immunity and survival induced by DC immunotherapy. Cancer Immunol Res. 2017;5:535–546. [PubMed: 28536100]
52. Pyonteck SM, Akkari L, Schuhmacher AJ, et al. CSF-1R inhibition alters macrophage polarization and blocks glioma progression. Nat Med. 2013;19:1264–1272. [PubMed: 24056773]
53. Priceman SJ, Sung JL, Shaposhnik Z, et al. Targeting distinct tumor-infiltrating myeloid cells by inhibiting CSF-1 receptor: combating tumor evasion of antiangiogenic therapy. Blood. 2010;115:1461–1471. [PubMed: 20008303]
54. Conway JG, Pink H, Bergquist ML, et al. Effects of the cFMS kinase inhibitor 5-(3-methoxy-4-((4-methoxybenzyl)oxy)benzyl) pyrimidine-2,4-diamine (GW2580) in normal and arthritic rats. J Pharmacol Exp Ther. 2008;326:41–50. [PubMed: 18434589]
55. Gao HM, Liu B, Zhang W, Hong JS. Novel anti-inflammatory therapy for Parkinson's disease. Trends Pharmacol Sci. 2003;24:395–401. [PubMed: 12915048]
56. Whitton PS. Neuroinflammation and the prospects for anti-inflammatory treatment of Parkinson's disease. Curr Opin Investig Drugs. 2010;11:788–794.
57. Moreno M, Bannerman P, Ma J, et al. Conditional ablation of astroglial CCL2 suppresses CNS accumulation of M1 macrophages and preserves axons in mice with MOG peptide EAE. J Neurosci. 2014;34:8175–8185. [PubMed: 24920622]
58. Parillaud VR, Lornet G, Monnet Y, et al. Analysis of monocyte infiltration in MPTP mice reveals that microglial CX3CR1 protects against neurotoxic over-induction of monocyte-attracting CCL2 by astrocytes. J Neuroinflammation. 2017;14:60. [PubMed: 28320442]
59. Klinkert K, Whelan D, Clover AJP, Leblond AL, Kumar AHS, Caplice NM. Selective M2 macrophage depletion leads to prolonged inflammation in surgical wounds. Eur Surg Res. 2017;58:109–120. [PubMed: 28056458]
60. Leblond AL, Klinkert K, Martin K, et al. Systemic and cardiac depletion of M2 macrophage through CSF-1R signaling inhibition alters cardiac function post myocardial infarction. PLoS ONE. 2015;10:e0137515. [PubMed: 26407006]
61. Cannarile MA, Weisser M, Jacob W, Jegg AM, Ries CH, Rüttinger D. Colony-stimulating factor 1 receptor (CSF1R) inhibitors in cancer therapy. J Immunother Cancer. 2017;5:53. [PubMed: 28716061]

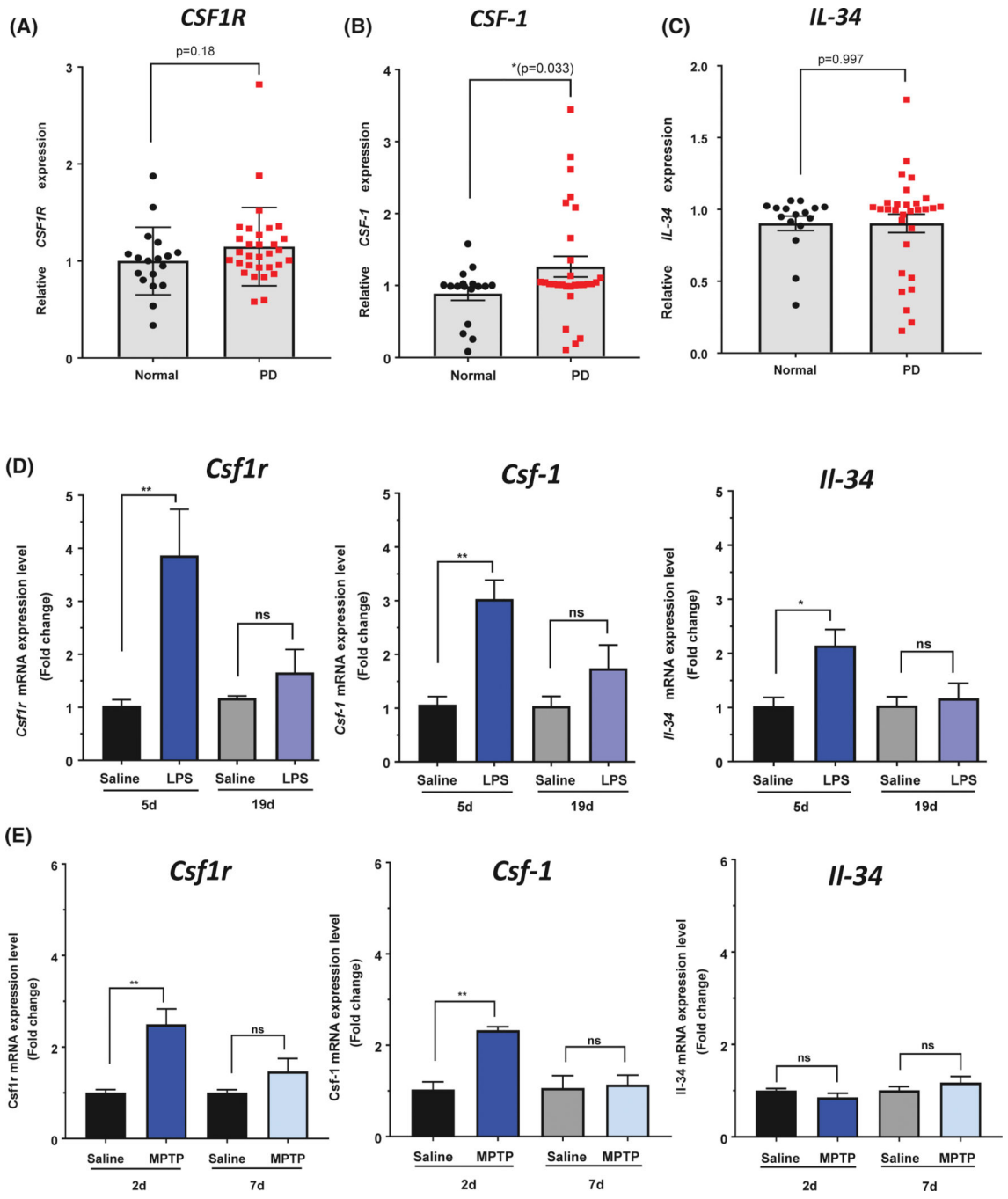

FIGURE 1.

Gene expression of CSF1R and its cognate ligands in the brain of PD patients and animal models of PD. Human gene expression of *CSF1R* (A), and *CSF-1* (B) were both increased in the SN of PD patients (n = 22 males and 9 females) compared to age-matched controls (n = 10 males and 7 females), whereas *IL-34* gene expression showed no difference (C). GEO numbers were normalized to 1 to generate relative expression values and allow comparison between datasets. D, Mice received LPS treatment (1 mg/kg) once daily for 4 days and sacrificed 1 or 14 days after the last injection. Quantitative PCR measurement of *Csf1r*,

Csf-1, and *Il-34* mRNA expression levels in the striatum of LPS-treated mice. E, Mice were treated with an acute MPTP paradigm and sacrificed 2 days or 7 days following the MPTP injections. Quantitative PCR measurements of *Csf1r*, *Csf-1,* and *Il-34* mRNA expression levels in the striatum of MPTP-treated mice. Data are represented as mean ± SEM, $*P < .05$, $**P < .01$, ns = not statistically significant $P > .05$

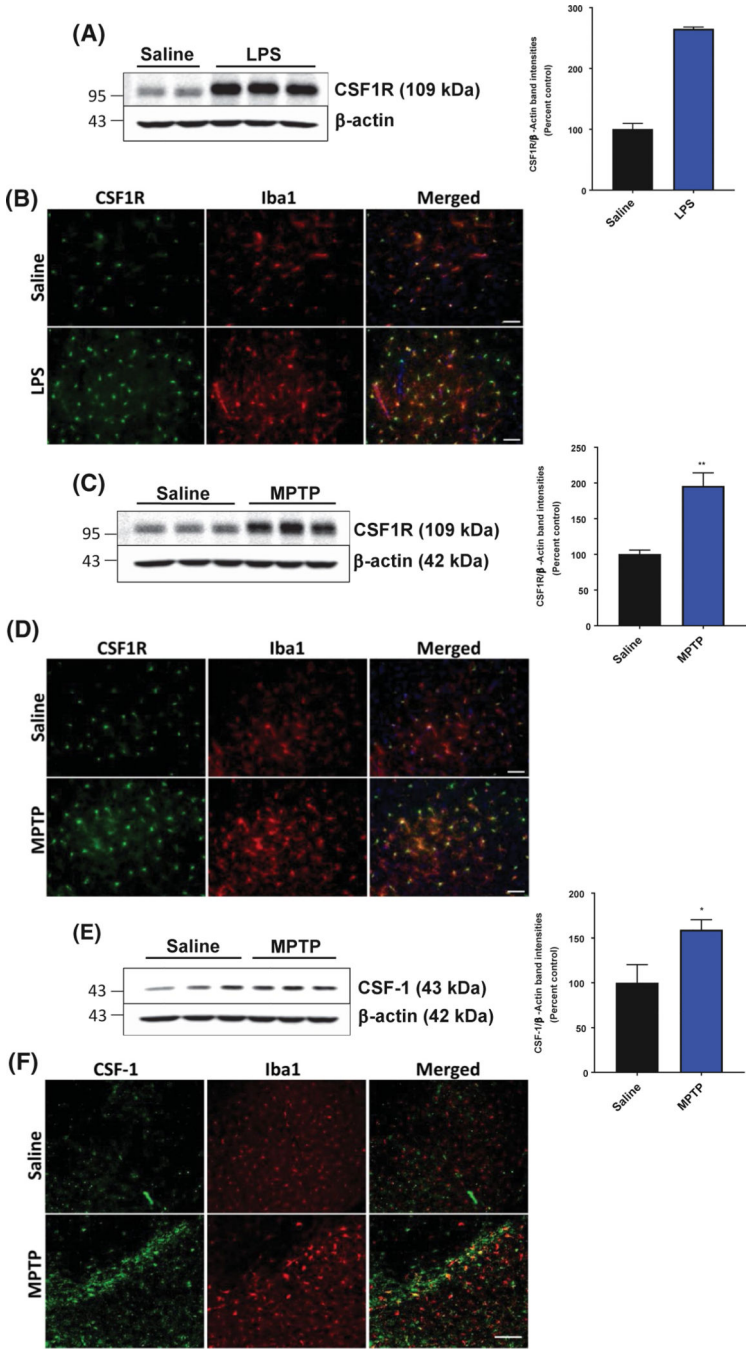

FIGURE 2.

CSF1R and CSF-1 protein levels are increased in the nigrostriatal pathway following neurotoxicant treatment. A and B, Increased protein level of CSF1R in the mouse striatum was treated with LPS by western blotting (A) and SN by immunofluorescent microscopy (B) (20× magnification, scale bar 50 μm). C and D, Increased protein level of CSF1R in the mouse striatum was treated with MPTP by western blotting (C) and SN by immunofluorescent microscopy (D) (20× magnification, scale bar 50 μm). E and F, Increased protein level of CSF-1 in the mouse striatum was treated with MPTP by western

blotting (E) and representative immunofluorescent microscopy images (F; 10× magnification, scale bar 40 μm) for CSF-1 (green) levels and Iba1-positive (red) cells of the SN following either saline or MPTP treatment. All data are presented as means ± SEM; n = 2–4 mice per group; *$P < .05$, **$P < .01$ and ***$P < .001$

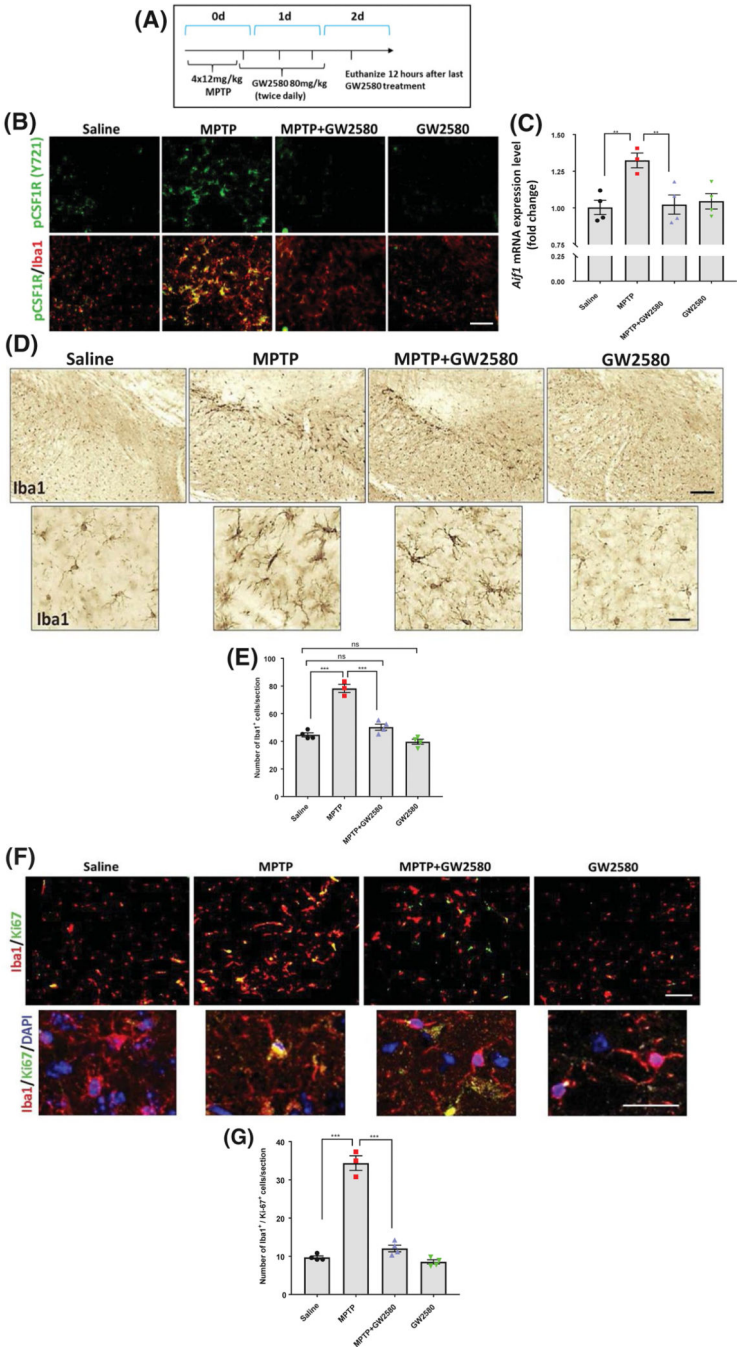

FIGURE 3.

Pharmacological inhibition of CSF1R with GW2580 attenuates MPTP-induced microglial proliferation without ablation of the basal microglia population. A, To measure neuroinflammation, animals were sacrificed 2 days after acute MPTP treatment. B, Representative immunofluorescent images of phosphorylated CSF1R (Y721) in green and Iba1 in red following MPTP and GW2580 treatment (scale bar, 40 μm). C, Gene expression of *Aif1* measured in the mouse striatum. D, DAB immunostaining of Iba1-positive cells in the SN following MPTP and GW2580 treatments (4.2× images, top panel; scale bar, 40 μm),

along with 40× magnification images for cellular morphology (bottom panel, scale bar 10 μm). E, Quantification of Iba1- positive cell numbers per section in the SN after MPTP and GW2580 treatments. F, Immunofluorescent staining of the SN for the cell proliferation marker Ki-67 (green) in Iba-1 positive (red) cells (10× magnification, scale bar 40 μm) with higher magnification (40× magnification, scale bar 25 μm) images including DAPI nuclear stain (blue). G, Total counts of Iba1-positive cells that were also positive for Ki-67 per section in the SN. All data are represented as mean ± SEM; n = 3–4 mice per group; $*P < .05$, $**P < .01$, $***P < .001$, ns = not statistically significant $P > .05$

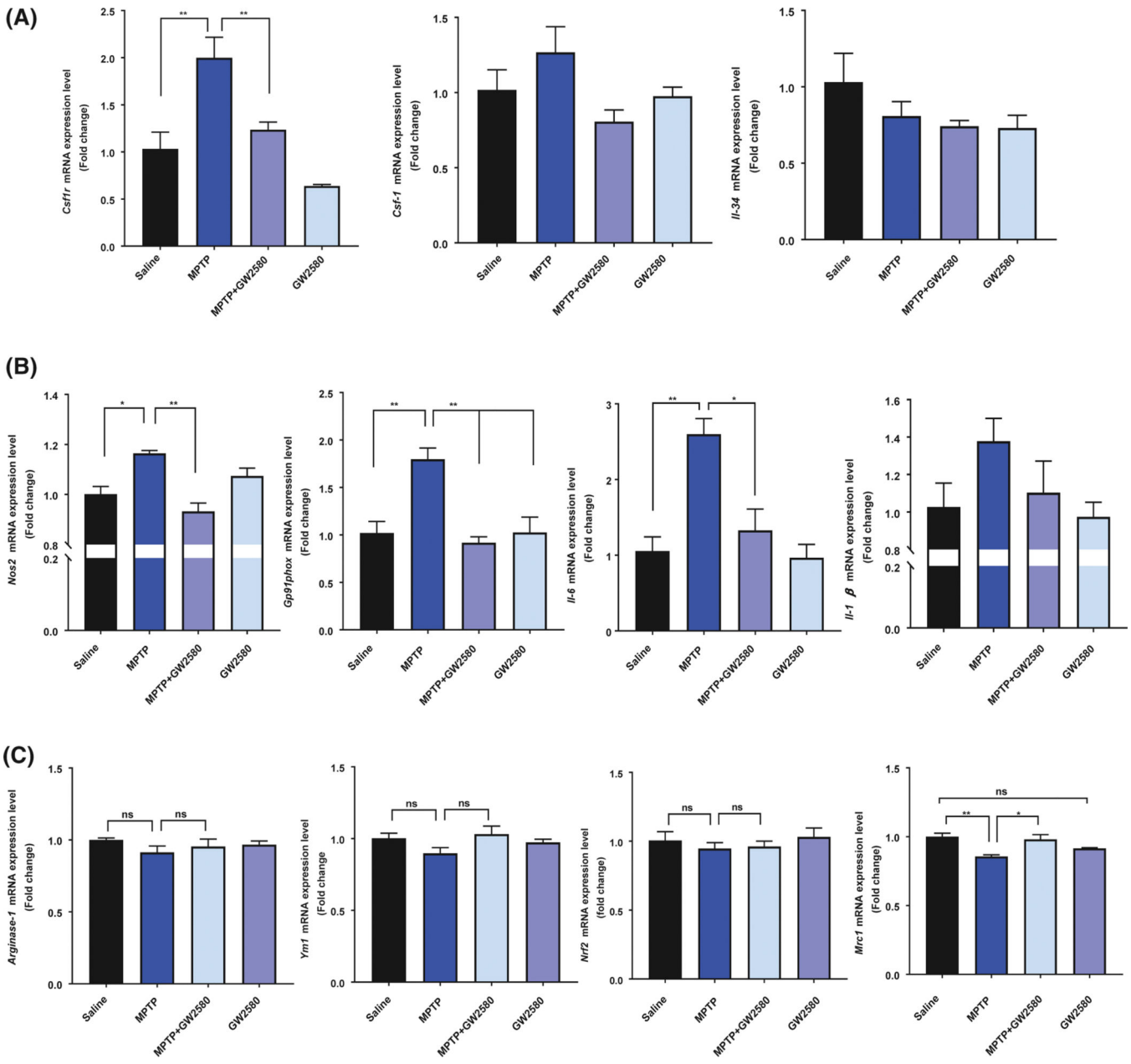

FIGURE 4.

GW2580 attenuates MPTP-induced tissue inflammatory response without reducing anti-inflammatory mRNA levels. A, Gene expression analysis of *Csf1r, Csf1,* and *Il-34* in the striatum 2 days following MPTP and GW2580 treatment. B, Gene expression analysis of the pro-inflammatory factors *Nos2, gp91phox, Il-6,* and *Il-1b* in the striatum 2 days following MPTP and GW2580 treatment. C, Gene expression analysis of the anti-inflammatory factors *Arginase-1, Ym1, Nrf2,* and *Mrc1* in the striatum 2 days following MPTP and GW2580 treatment. All data are represented as mean ± SEM; n = 3–4 animals per group; $*P < .05$, $**P < .01$, ns = not statistically significant

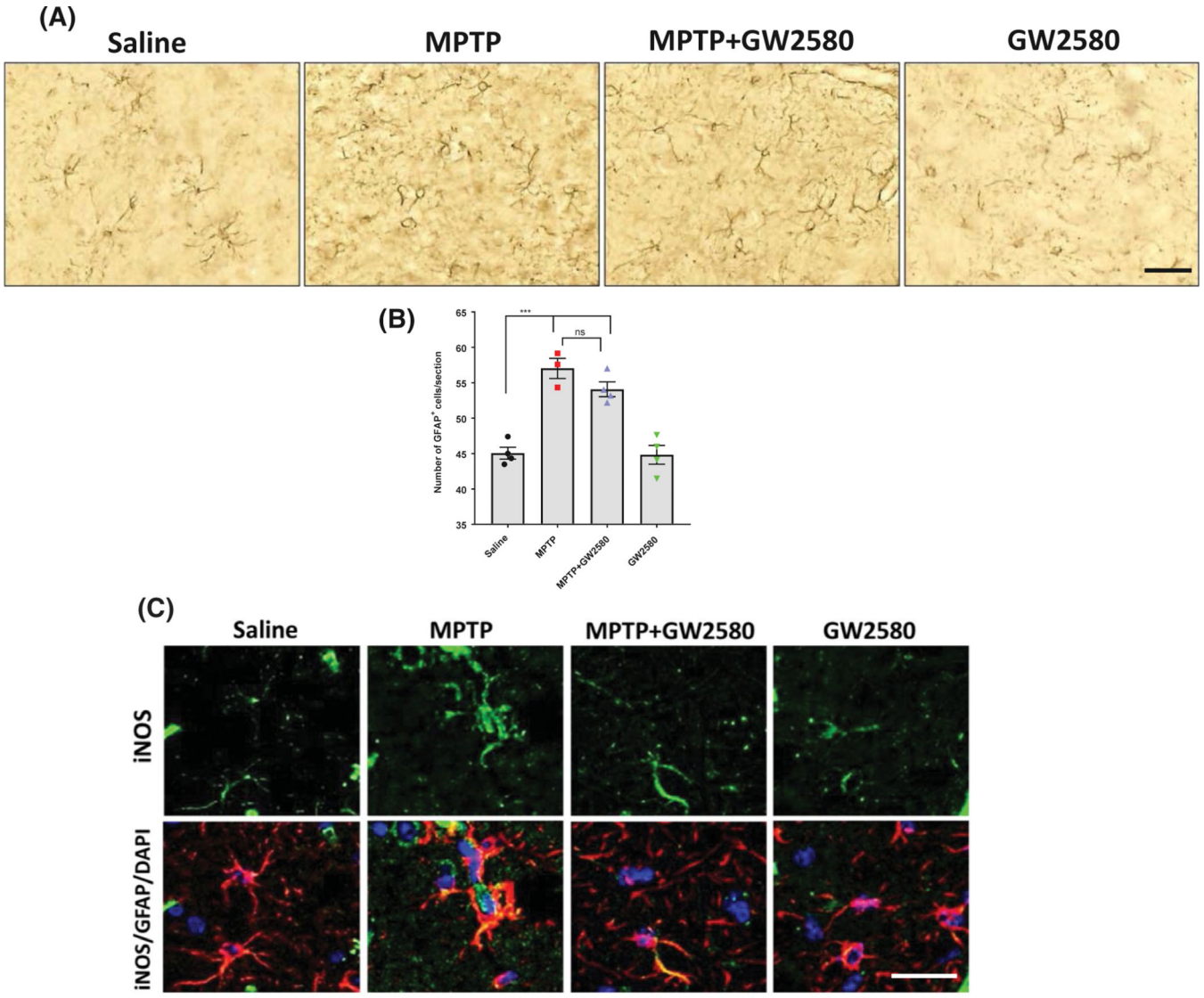

FIGURE 5.

Pharmacological inhibition of CSF1R with GW2580 does not alter astrocyte reactivity. A and B, Representative DAB immunostaining images (20× magnification, scale bar 40 μm) for GFAP-positive cells (A) and total GFAP-positive cell counts (B) in the SN after MPTP and GW2580 treatment. C, Representative immunofluorescent images (40× magnification, scale bar 25 μm) for iNOS (green) in GFAP-positive cells (red) with DAPI stained nucleus (blue). All data are represented as mean ± SEM; n = 3–4 animals per group; ***$P < .001$, ns = not statistically significant

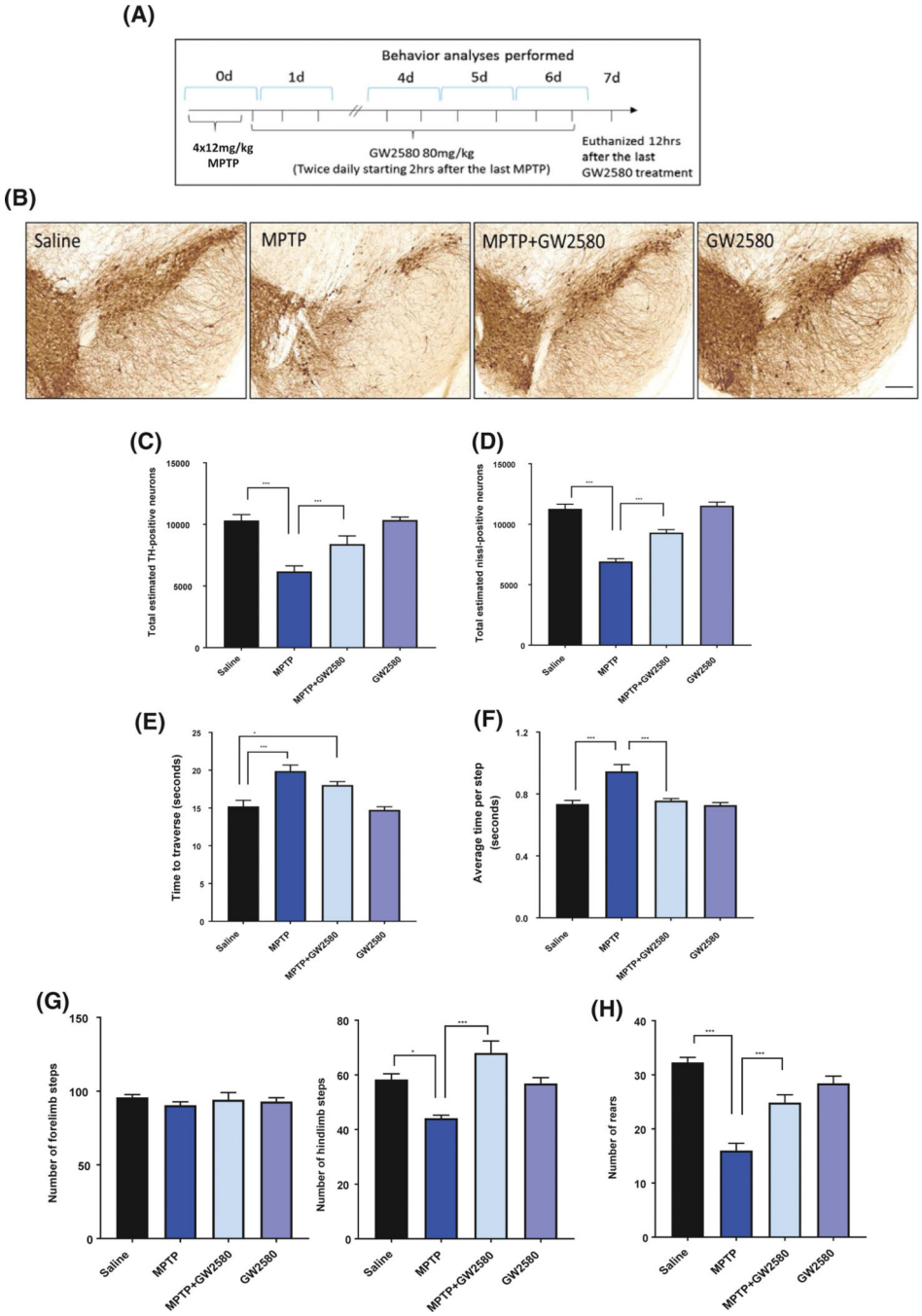

FIGURE 6.

GW2580 treatment improves MPTP-induced dopaminergic neurotoxicity and motor dysfunction. A, To measure dopaminergic neurotoxicity and behavioral deficits animals were sacrificed 7 days after acute MPTP treatment, with behavioral training occurring on day 4–5 and measurements taken on days 6. B, Representative DAB immunostaining images for the dopaminergic neuron marker tyrosine hydroxylase (TH) at 4.2×, scale bar 100 μm. C and D, Unbiased stereological counting of TH-positive (C) and Nissl-positive (D) neurons in the SN following MPTP and GW2580 treatment. E and F, Analysis of motor dysfunction

following MPTP and GW2580 treatment by averaging 5 trials measuring total time taken to traverse a challenging beam (E), and average time per step (F) on the challenging beam. G and H, Spontaneous activity measurements of total rearing events (G), total number of forelimb steps (H, left panel), and total number of hindlimb steps (H, right panel) after MPTP and GW2580 treatment. All data are represented as mean ± SEM; n = 5–6 animals per group; $*P < .05$, $**P < .01$, and $***P < .001$